Improvement of optical trapping effect by structuring the illuminating laser beam

S. Haddadi, K. Ait-Ameur

Version of Record: https://www.sciencedirect.com/science/article/pii/S0030402621019422
Manuscript_f6d0eaf8252441019a07337e7c308aa4

Improvement of optical trapping effect by structuring the illuminating laser beam

S. Haddadi[1], K. Ait-Ameur[2]

[1]: Centre de Développement des Technologies Avancées, Division Milieux Ionisés et Lasers, P.O. Box 17, Baba-Hassan, 16303 Algiers, Algeria.

[2] : Centre de Recherche sur les Ions, les Matériaux et la Photonique (CIMAP), UMR 6252 CEA-CNRS-ENSICAEN-Université de Caen, 6 Bd Maréchal Juin, 14050 Caen cedex 4, France.

Corresponding author: kamel.aitameur@ensicaen.fr

REVISED VERSION

Abstract: We have considered the negative influence of spherical aberrations (SA) on longitudinal and transversal forces occurring in optical tweezers based on a focused Gaussian beam (GB). We have shown that, for a given power and incident beam width, the replacement of the usual GB by a "rectified" LG_{p0} (one peak surrounded by p rings having the same sign) improves the longitudinal force by a factor ranging from (p+1) to (p+2). The "rectification" of a LG_{p0} beam is assumed to be done by a binary diffractive optical element which transforms the negative rings into a positive one.

1. Introduction

Optical trapping based on the use of one or several laser beams is a field having received much attention since the early 1970s when the pioneer Arthur Ashkin (Nobel prize in Physics 2018) laid the foundation stone of this discipline [1,2]. This seminal work has given a significant number of applications of the single-beam gradient force optical trap also called as optical tweezers [3]. These applications encompass both physics and biology. For a survey of the literature dedicated to optical tweezer applications see Ref. [4,5]. The modelling of the interaction between a small particle and a laser beam is different depending on the ratio between the particle size and the wavelength λ of the trapping laser beam. For sake of simplicity, we will assume a spherical dielectric particle of radius a. Usually, three cases can be distinguished:

- Geometrical optics regime ($a >> \lambda$)
- Generalised Lorenz-Mie regime ($a \approx \lambda$)
- Rayleigh regime ($a << \lambda$). In this regime, the particle is treated as a point dipole subject to the laser electrical field. The latter, for the sake of simplicity, is assumed to have the cylindrical symmetry around the direction of propagation $\hat{z}$.

In the following, we are considering the Rayleigh regime that is involved when trapping nanoparticles. In this regime, since $a << \lambda$ it is reasonable to admit that the electrical field $\vec{E}$ of the laser light is uniform inside the nanosphere. It results in an induced dipole having a dipole moment $\vec{p}$ given by

$$\vec{p} = \alpha \vec{E} \tag{1}$$

where α is the polarisability of the particle, given by the Clausius-Mossotti relation [5]

$$\alpha = 4\pi\varepsilon_0 a^3 n_m^2 \left[\frac{m^2 - 1}{m^2 + 2} \right] \tag{2}$$

where $m = n_p / n_m$ is the ratio of the refractive index of the particle n_p and the surrounding mdium n_m. In the dipole approximation ($a << \lambda$) there are two relevant forces exerted by light on the particle [6]: a scattering force and a gradient force.

The time-averaged gradient force $\vec{F}_{grad}$ is given by

$$\vec{F}_{grad} = <(\vec{p}\vec{\nabla})\vec{E}>_t = \frac{1}{2}\alpha\vec{\nabla}\left|\vec{E}\right|^2 \tag{3}$$

By definition, the intensity $I(\rho,z)$ of the laser beam is the time-averaged of the Poynting vector modulus which takes the following form

$$I(r,z)=\frac{1}{2}\varepsilon_0 n_m c\left|\vec{E}(r,z)\right|^2 \tag{4}$$

where r (z) is the radial (longitudinal) coordinate, and c the speed of light in vacuum. Note that it is important to distinguish between the "true" intensity given by Eq. (4) and the optical intensity usually expressed by $\left|\vec{E}(r,z)\right|^2$.

By considering Eq. (2) and (4), the gradient force can be written as follows

$$\vec{F}_{grad}=\frac{4\pi a^3}{c}\left[\frac{m^2-1}{m^2+2}\right]\vec{\nabla}I(r,z) \tag{5}$$

The gradient operator $\vec{\nabla}$ can be written as the sum of longitudinal and transverse components:

$$\vec{\nabla}=\vec{\nabla}_z+\vec{\nabla}_r \tag{6}$$

As pointed out above, the nanosphere acts like an oscillating dipole, and consequently will radiate an electromagnetic wave in all directions that causes a momentum transfer to the particle. A force is involved in this transfer which is called as scattering force $\vec{F}_{scat}$ pushing the particle along the direction of propagation of the laser beam:

$$\vec{F}_{scat}=\frac{128\pi^5 n_m a^6}{3c\lambda^4}\left[\frac{m^2-1}{m^2+2}\right]^2 I(r,z)\hat{z} \tag{7}$$

The criterion for realising the axial stability [3] of the single-beam trap is $F_{grad}>F_{scat}$. This condition is fulfilled provided strong intensity gradients are achieved, and that necessitates a highly focused laser beam. This objective is severely obstructed by the presence of spherical aberration originating from the two following causes:

(i) A tight focusing involves significant spherical aberration due to the high numerical aperture of the utilised focusing microscope objective. Such spherical aberration can be corrected by construction. Generally, optical tweezers usually involve the use of an oil-immersion objective allowing high values of the numerical aperture (NA). Note that in this paper we do not wish to be in the case of a tight focusing for several reasons discussed in Section 2.

(ii) Spherical aberration will be introduced as a result of the mismatch in the refractive indices between objective oil and water when the trapped particle is suspended in a water solution [7-9].

Since, broadly speaking the effect of spherical aberration on the focusing properties is a diminution of the focused intensity, we can expect that the trapping force will decrease [10,11]. As a consequence, for keeping high the trapping force in optical tweezers a strategy of spherical aberration compensation has been implemented by quite a lot researchers [12-15]. In Section 2, we will revisit the properties of an optical tweezer enlighten by a pure Gaussian beam and an aberrated Gaussian beam. In Section 3, we will propose the use of rectified LG_{p0} beam as the laser beam trapping in order to reduce the negative influence of spherical aberrations. Note that it has been recently demonstrated that the focusing of a rectified radial Laguerre-Gauss beam (one peak surrounded by p rings of light) is very little sensitive to spherical aberration [16]. The operation of "rectification" of a LG_{p0} beam is achieved by using a binary Diffractive Optical Element (DOE) which transforms the negative rings into a positive one. As a result, the focused intensity profile is quasi-Gaussian in shape [16].

2. Properties of optical trapping effect by using an aberrated Gaussian beam

The geometry of the Gaussian beam focusing is given in Fig. 1. The incident collimated beam on the focusing lens is a Gaussian with a width W_1 is characterised by its electric field distribution given by

$$E_{in}(\rho) = E_0 \exp[-\rho^2 / W_1^2] \tag{8}$$

where ρ is the radial coordinate in the plane of the lens of focal length f_L. Note that the objective of this paper is to prove that the replacement of the Gaussian beam by a rectified Laguerre-Gaussian beam allows to reduce the bad influence of spherical aberration on the performance of optical tweezers. Therefore we are not looking for a tight focusing and this is why for the numerical calculations we will set the value of the focal length of the focusing lens to f_L=50 mm with a numerical aperture equal to 0.3. There are at least two other reasons for this choice: first, the use of the same parameters as in Ref. [16] for reference purpose, and secondly for legitimating the use of the Fresnel-Kirchhoff integral for determining the diffraction fields in the framework of the paraxial approximation. For all calculation the

wavelength is $\lambda = 1064\,nm$. Note that obtening a tight focusing is always a challenge that continues today for a variety of laser beams (Gaussian, vortex,…) [17-19].

In Fig. 1, the primary spherical aberration (SA) is supposed, for sake of simplicity, set against the focusing lens. The complex transmittance τ_L of the lens in the framework of the paraxial approximation is given by the following expression

$$\tau_L = \exp[i\phi(\rho)] \tag{9}$$

$$\text{With} \quad \phi(\rho) = \frac{2\pi}{\lambda}\left(\frac{\rho^2}{2f_L} - W_{40}\frac{\rho^4}{\rho_0^4}\right) \tag{10}$$

where λ is the laser beam wavelength, W_{40} is the spherical aberration coefficient expressed in units of wavelength of light, $\rho_0 = NA \times f_L$ is the lens radius and NA=0.3 its numerical aperture. Since $\rho_0 > 3.5W_1$, we can overlook any beam clipping.

In the next, we will determine the main characteristics of the optical forces exercised over a dielectric nanoparticle with and without spherical aberration.

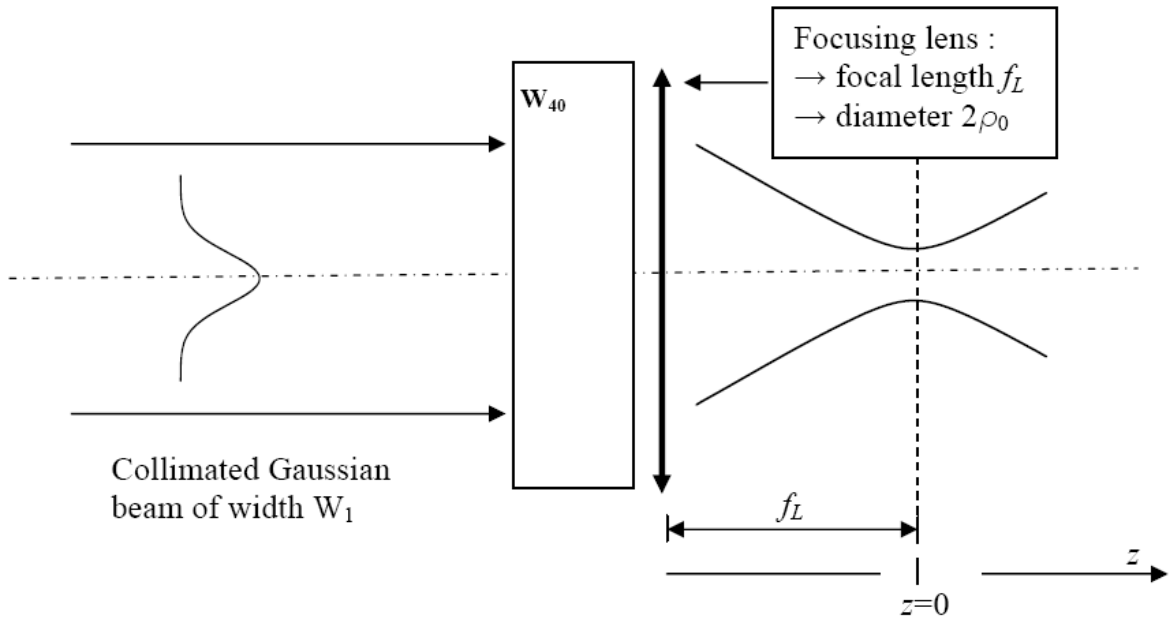

Figure 1: Set-up showing the geometry of the diffraction of a collimated Gaussian beam traversing a spherical aberration and a lens of diameter $2\rho_0$.

2.1 Optical tweezer without spherical aberration ($W_{40}=0$):

We will assume the Rayleigh distance of the incident Gaussian beam (GB) to be very large compared to the focal length, i.e. $(\pi W_1^2/\lambda) >> f_L$. This implies that the beam-waist of the focused GB is located at location $z=0$ coincides with the geometrical focal plane of the lens. In these conditions, the width W_0 of the beam-waist is given by

$$W_0 = \frac{\lambda f_L}{\pi W_1} \tag{11}$$

and the longitudinal variations of the GB width obeys the well known relation

$$W(z) = W_0\sqrt{1+\left(\frac{z}{z_0}\right)^2} \tag{12}$$

where $z_0 = \pi W_0^2/\lambda$ is the Rayleigh distance of the focused GB. The optical intensity distribution $\left|\vec{E}(r,z)\right|^2$ of the focused GB is given by

$$\left|E(r,z)\right|^2 = E_0'^2 \times \left(\frac{W_0}{W(z)}\right)^2 \times \exp\left[-2r^2/W^2(z)\right] \tag{13}$$

where r is the radial coordinate associated with the focused GB and the on-axis intensity $E_0'^2$ is related to E_0^2 the incident on-axis intensity by the following energy conservation formula

$$E_0'^2 = E_0^2 \times \frac{W_1^2}{W_0^2} \tag{14}$$

If we look at Eqs. (5) and (7), it is seen that the gradient and scattering forces can be written in the following form

$$\vec{F}_{grad} = K_1 \times \vec{\nabla}\left(\left|\vec{E}(r,z)\right|^2\right) \tag{15}$$

$$\vec{F}_{scat} = K_2 \times \left|\vec{E}(r,z)\right|^2 \tag{16}$$

where K_1 and K_2 are coefficients easily deductible. These coefficients do not depend on the diffraction effects induced by the spherical aberration. Consequently, it is legitimate to regard the possible loss of trapping stability by considering the variations of ratio R versus W_{40}. The ratio R is defined by

$$R = \frac{-\left[\hat{z}.\vec{\nabla}_z\left(\left|\vec{E}(0,z)\right|^2\right)\right]_{\min}}{\left[\left|\vec{E}(0,z_{\min})\right|^2\right]} \qquad (17)$$

where $z_{\min}$ is the position where the longitudinal gradient is minimum. In the above equation, ratio R is proportional to the ratio of the backward axial gradient force to the forward scattering force

The longitudinal gradient of the optical intensity for $W_{40} = 0$ is given by

$$\hat{z}.\vec{\nabla}_z\left(\left|\vec{E}(0,z)\right|^2\right) = \frac{-2E_0'^2 z_0 z}{(z_0^2 + z^2)^2} \qquad (18)$$

The function $\hat{z}.\vec{\nabla}_z\left(\left|\vec{E}(0,z)\right|^2\right)$ has a maxima (minima) located at $z_{\max} = -z_0/\sqrt{3}$ ($z_{\min} = +z_0/\sqrt{3}$) and given by

$$D_{norm} = \left[\hat{z}.\vec{\nabla}_z\left(\left|\vec{E}(0,z)\right|^2\right)\right]_{\max} = -\left[\hat{z}.\vec{\nabla}_z\left(\left|\vec{E}(0,z)\right|^2\right)\right]_{\min} = \frac{-\sqrt{27}\lambda W_1^2 E_0^2}{8\pi W_0^4} \qquad (19)$$

In the following, the numerical value of longitudinal and transversal gradients of the optical intensity will be normalised by the quantity D_{norm} defined for $W_{40} = 0$. This allows to easily see the degradation or the improvement of the gradient and scattering forces according to the variations of W_{40} the SA coefficient. Likewise, the numerical value of the optical intensity in any case will be normalised by $\left[\left|\vec{E}(0, z_0/\sqrt{3})\right|^2\right]$ for $W_{40} = 0$, the value of reference for the pure Gaussian beam.

2.2 Optical tweezer with spherical aberration ($W_{40} \neq 0$):

Before proceeding, it is important to have a global vision of the intensity distribution around the focal region of a Gaussian beam focused and subject to a spherical aberration. In Fig. 2 is plotted the two dimensional intensity distribution (longitudinal and transversal) for W_{40}=0 and W_{40}=10λ. In the presence of spherical aberration we observe several effects: (i) a widening of the focal volume accompanied by an intensity reduction, (ii) the maximum of intensity is shifted toward the lens, and (iii) a deformation of the radial intensity distribution which is no longer Gaussian especially before the geometrical focal plane, i.e. for z<0. All these phenomena contribute to reduce the efficiency of optical tweezers in presence of a spherical aberration as it will be shown below.

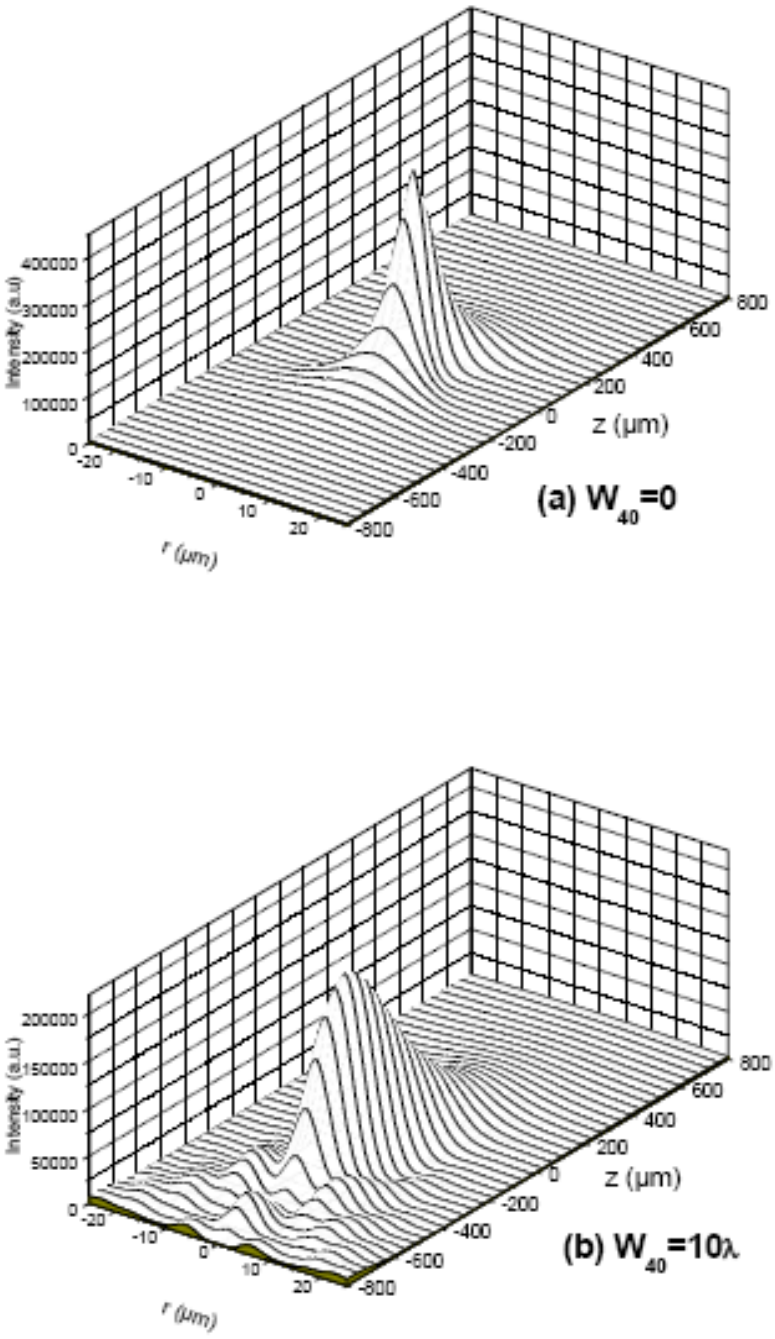

Figure 2: Two-dimensional intensity distribution of a Gaussian beam of width $W_1 = \sqrt{11}\,mm$ focused by a lens of focal length $f_L = 50\,mm$ for (a) W_{40}=0 and (b) W_{40}=10λ. Note that the position $z = 0$ corresponds to the geometrical focus of the lens.

Usually, in diffraction problems we consider separately the longitudinal and transversal effects in order to improve the description accuracy. With that in mind, the on axis-intensity $|E(0,z)|^2$ is plotted versus z the longitudinal position in Fig. 3 for several values of W_{40} the SA coefficient. As expected, the effect of the SA on the focusing of a Gaussian beam include two aspects:

(i) In Fig. 3-a, one observes that the position $z_{\max}$ of the best focus (maximum of the on-axis intensity) is shifted toward the lens for $W_{40} > 0$. That is why we defined a focal length f_{40} associated with the SA [16]

$$f_{40} = \frac{\rho_0^2}{4\sqrt{3}\lambda W_{40}} \tag{20}$$

The position of the best focus should obey to the following equation

$$\frac{1}{z_{\max}} = \frac{1}{f_L} + \frac{1}{f_{40}} \tag{21}$$

(ii) In Fig. 3-a it is seen that as W_{40} is increased, the intensity of the best focus decreases while the depth of focus (DoF) increases. The DoF can be defined as the width of the on-axis intensity distribution.

It is important to note that focusing a GB subject to SA does not lead systematically to a lower intensity in the focal point compared to aberration-free focusing. Indeed, it has been demonstrated [20] that a lens with negative SA can achieve a smaller focused beam radius, a larger maximum of the on-axis intensity $|E(0,z)|^2$ than without SA. For a positive SA, one get exactly the opposite, that is to say a larger focused beam radius and a smaller maximum focused on-axis intensity. However, in the latter case if some hard clipping is added, it can result in a stronger focus [21].

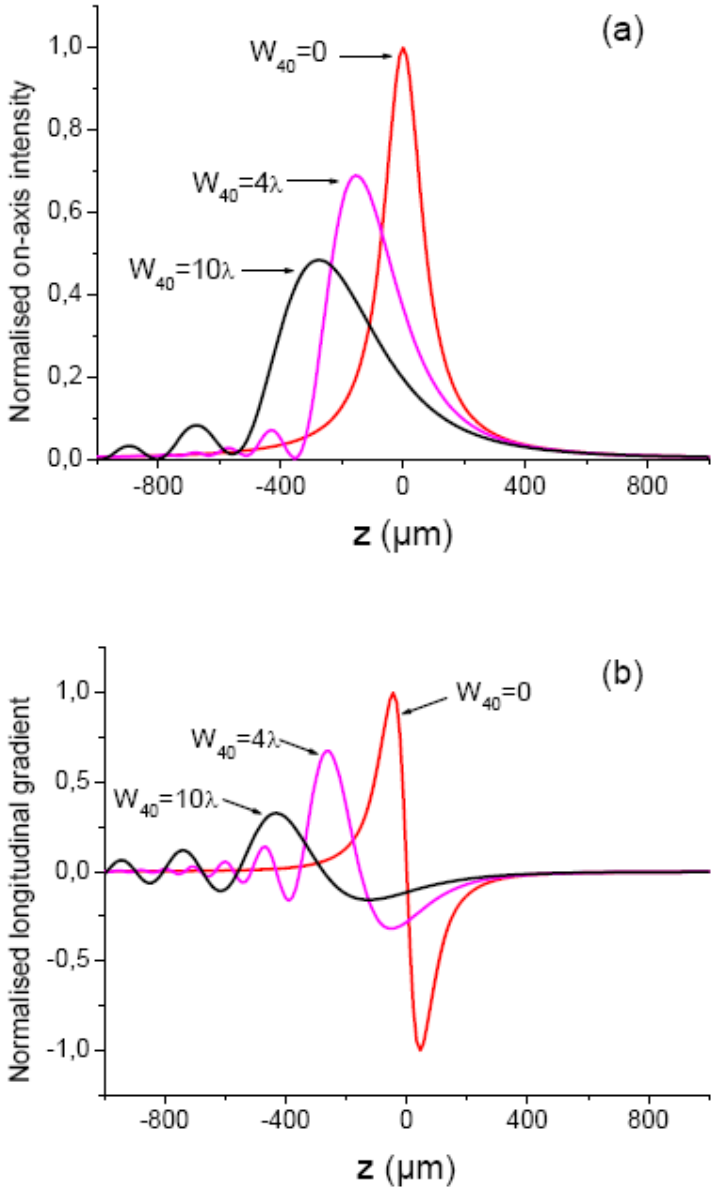

Figure 3: **(a)** Variations of the normalised on-axis intensity distribution versus the longitudinal position. **(b)** Variation of $\hat{z}.\vec{\nabla}_z\left(\left|\vec{E}(0,z)\right|^2\right)$ the longitudinal gradient of the on-axis intensity versus the longitudinal position. The incident Gaussian beam of width $W_1 = \sqrt{11}\,mm$ is focused by a lens of focal length $f_L = 50\,mm$ for several values of W_{40} the spherical aberration coefficient. Note that the position $z = 0$ corresponds to the geometrical focus of the lens.

Fig.3-b shows the variation of $\hat{z}.\vec{\nabla}_z\left(\left|\vec{E}(0,z)\right|^2\right)$ the longitudinal gradient of the on-axis intensity for several values of W_{40}. For $W_{40}=0$, the longitudinal gradient is symmetric with respect to the origin $z=0$. The plots in Fig.3-b are no longer symmetrical for $W_{40}\neq 0$. It is observed that the longitudinal gradient force pointing toward the z<0 direction is smaller than that oriented in the z>0 direction. As a result, this effect can threaten the stability of the trap. The stability of the optical trap can be described by using the ratio R defined by Eq. (17) and plotted versus W_{40}.in Fig. 4. Before interpreting the plot of Fig. 4, we must first remark that the stability condition of the optical trap is expressed by the following inequality

$$R_F=\left|\vec{F}_{grad,z}(z_{\min})\right|/\left|\vec{F}_{scat}(z_{\min})\right|>1 \qquad (22)$$

Let R_{F0} the value of R_F for the ideal optical tweezer, i.e. for $W_{40}=0$. The necessary condition for keeping a trapping capacity is $R_{F0}\times R>1$. For instance, if $R_{F0}=2$ then from fig.5 we deduce that the trap remains stable if $W_{40}<3.1\lambda$.

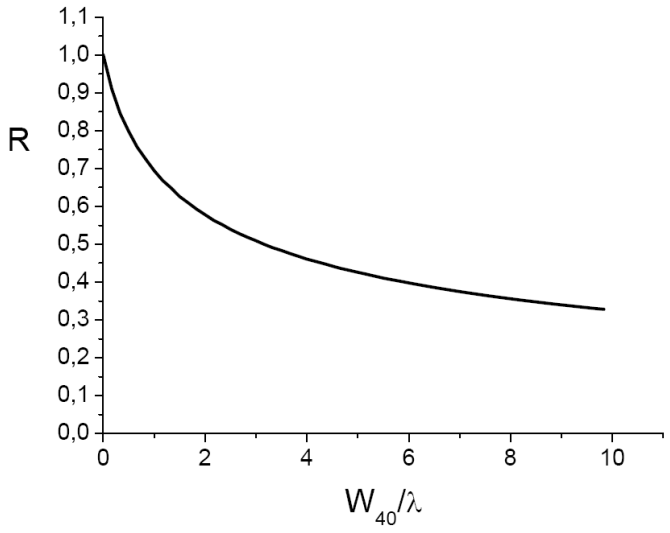

Figure 4: Variations of the ratio $R=-\left[\hat{z}.\vec{\nabla}_z\left(\left|\vec{E}(0,z)\right|^2\right)\right]_{\min}/\left[\left|\vec{E}(0,z_{\min})\right|^2\right]$ versus W_{40} the SA coefficient.

3. Enhancing the efficiency of an optical tweezer

As pointed out above, mitigation of the spherical aberration is fundamental for maintaining a high quality in the trapping laser beam focusing [12-15]. The aim of this paper is to propose a new strategy for reducing the effect of SA on the focus quality and that for the sake of enhancement of the trapping forces. In the next, instead of the usual Gaussian beam, we will consider as input laser beam in Fig. 1 two families of laser beams. The first one is the radial Laguerre-Gauss beams LG_{p0} made up of a central peak surrounded by p rings of light. The second one noted $R-LG_{p0}$ results from the "rectification" of a LG_{p0} beam. The operation of rectification of a LG_{p0} beam by a binary diffractive optical element (BDOE) consists to transform the rings having a negative electric field into a positive one. The $R-LG_{p0}$ beams have been considered through several papers [22-25] where the BDOE used is described in detail, and will be not repeated here. There are three key points to remember about the properties of a focused $R-LG_{p0}$ beam which is made up, at the lens input, of a central peak surrounded by p positive rings of light. The first one is that a focused $R-LG_{p0}$ beam give rise to a single-lobed intensity profile in the focal plane of the focusing lens [22,23]. The second one is that a $R-LG_{p0}$ beam is less sensitive than the LG_{00} beam to a spherical aberration in comparison with the usual GB [16]. The third one is the possibility to produce a single-lobed focal spot with a central intensity of about p times the intensity produce by the focusing of a GB having the same power and same width based on the second-order intensity moment [26]. One can expect that a $R-LG_{p0}$ beam, characterised by a given power and a given width based on second-order intensity moment, could be superior to the usual Gaussian beam, having the same characteristics, for achieving an optical tweezer. On the other hand, some authors have considered the use of Laguerre-Gauss beams in trapping of particles [27-33], but very little attention has been devoted to focusing of LG_{p0} beams subject to spherical aberration. To the best of our knowledge, this is the first comparative study of performances of optical tweezers using LG_{p0} and $R-LG_{p0}$ beams subject to spherical aberration that is presented hereafter.

Before proceeding, let us define the electric fields associated with LG_{p0} and $R-LG_{p0}$

$$LG_{p0}\text{ beam:}\quad E_{in}(\rho)=E_{p0}\times Lp(2\rho^2/W_{p0}^2)\times\exp[-\rho^2/W_{p0}^2] \tag{23}$$

$$R-LG_{p0}\text{ beam:}\quad E_{in}(\rho)=E_{p0}\times\left|L_p(2\rho^2/W_{p0}^2)\right|\times\exp[-\rho^2/W_{p0}^2] \tag{24}$$

where L_p is the Laguerre polynomial of order p (p=0-5), and W_{p0} is the width of the Gaussian term. We will impose two essential requirements to the LG_{p0} and $R-LG_{p0}$ beams. First, they carry the same power, and secondly they have the same width based on the second-order intensity moment. These two requirements are satisfied [16] if one takes the following parameters appearing in Eq. (23) and (24)

$$E_{p0} = E_{00} \times \sqrt{2p+1} \tag{25}$$

$$W_{p0} = \frac{W_{00}}{\sqrt{2p+1}} \tag{26}$$

All the beams, whatever the mode order p have the same width $W_{p0} \times \sqrt{2p+1} = W_{00}$, where W_{00} is the width of the LG_{00} Gaussian beam. The need for equal beam width whatever the mode order p is dictated by the presence of spherical aberration which increases with ρ^4 as shown in Eq. (10). Likewise, the beam power has to be the same for all beams otherwise we cannot compare the trapping forces.

Although the Gaussian beam is generally considered as the ideal laser beam for optical tweezers, it could be considered that the use of LG_{p0} beam is incongruous since its intensity profile after focusing is made up of several rings. However, this approach is wrong since the trapping of a nanoparticle does not directly involve the whole beam profile but rather the local longitudinal and transversal gradients of intensity. In addition, it is important to note that a rectified LG_{p0} beam after focusing leads to a quasi-Gaussian intensity profile free from any rings [22,23]. It will be shown in the next Sections that a rectified LG_{p0} beam compared to a Gaussian beam having the same width and power can show a higher performance in term of trapping force. In the following, the study of optical forces will be divided into two parts: longitudinal and transversal forces. Before going into details let us examine the plots in Fig. 5 displaying the variations of the on-axis intensity and longitudinal gradient when the incident light is a rectified LG_{50} beam subject to a spherical aberration W_{40}=0, 4λ and 10λ. The comparison between Fig. 3 and 5 demonstrates clearly that the stability of the tweezers for a rectified LG_{50} beam is more resistant against the spherical aberration than the Gaussian beam. Indeed, unlike the Gaussian enlightening (Fig.3-b) the longitudinal gradient force is relatively

symmetric on both sides of the focal plane for the rectified LG_{50} beam (Fig. 5-b) which augurs well for a good trapping stability. In the next, we will see the role of the mode order p of the incident LG_{p0} beam on the tweezers performances when subject to a spherical aberration.

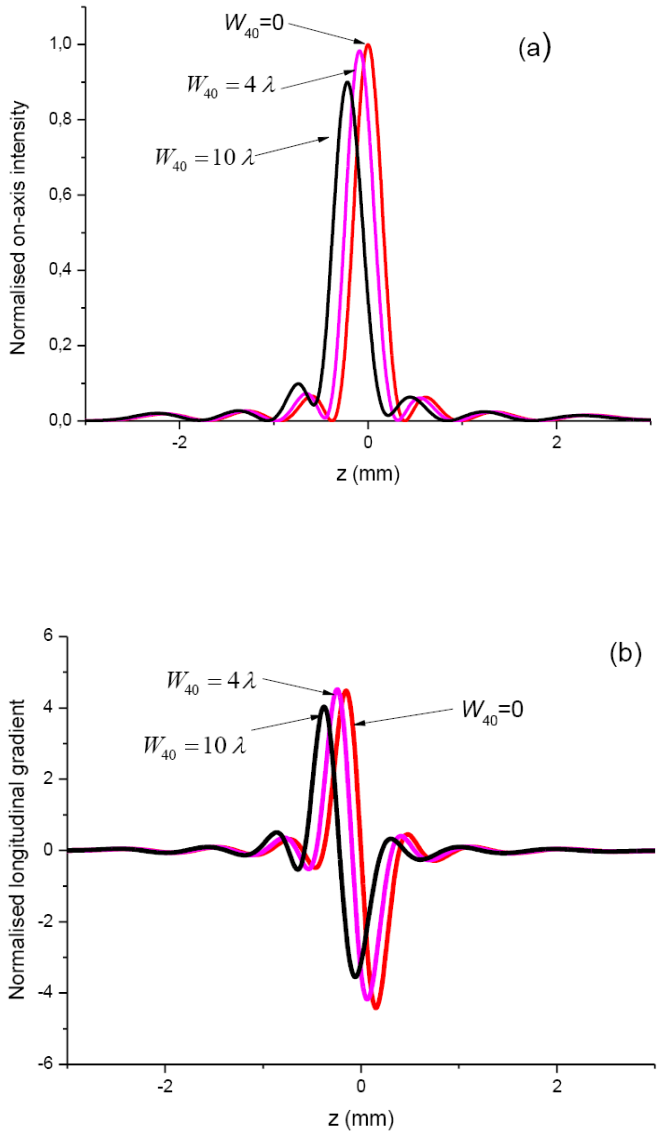

Figure 5: **(a)** Variations of the normalised on-axis intensity distribution versus the longitudinal position. **(b)** Variation of $\hat{z}.\vec{\nabla}_z\left(\left|\vec{E}(0,z)\right|^2\right)$ the longitudinal gradient of the on-axis intensity versus the longitudinal position. The incident light is a rectified LG_{50} beam having the same width and power than the Gaussian beam in Fig. 3.Note that the position $z=0$ corresponds to the geometrical focus of the lens.

3.1 Longitudinal optical forces

As before for the Gaussian beam in Section 2, we will introduce in Eq. (27) a normalised ratio Z_p associated with a LG_{p0} or ${}^{R}LG_{p0}$ beam as input of the focusing lens,

$$Z_p = \frac{\{R_F\}_{p>0}^{W_{40}>0}}{\{R_F\}_{p=0}^{W_{40}=0}} \tag{27}$$

The ratio Z_p is defined as the value of R_F normalised by the value of R_F (see Eq. (22)) determined for a LG_{00} input without spherical aberration ($W_{40}=0$). Depending on the magnitude of ratio Z_p, it can be seen if the efficiency of the optical trapping force is improved ($Z_p>1$) or not improved ($Z_p<1$) compared to the case of a Gaussian beam enlightening. The results are shown in Fig. 6-a for a pure LG_{p0} beam and in Fig. 6-b for a rectified LG_{p0} beam. It is seen in Fig.6-a that replacing the usual Gaussian beam by a pure LG_{p0} beam improves very little the enhancement of the ratio Z_p which can be considered as a figure of merit of the optical tweezers. In contrast, when the enlightening beam is a rectified LG_{p0} beam Fig. 6-b shows clearly that the improvement of Z_p the longitudinal figure of merit of the optical tweezers. Indeed, it is seen that without SA ($W_{40}=0$) the factor by which the ratio Z_p for a Gaussian beam enlightening is multiplied varies from (p+1) until (p+2). It is important to remember that all the LG_{p0} beams, for p=0 to 5, have the same power and the same width based on the second-order intensity moment as expressed through Eqs. (25) and (26). In addition, it is seen in Fig. 6 that the figure of merit Z_p is resilient to the SA as much as the mode order p is high. For instance, the relative variation of Z_p for a LG_{00} ($R-LG_{50}$) input is about -56% (-8.7%) when the SA coefficient W_{40} varies from 0 to 5λ. It is clear that using a rectified LG_{p0} as input beam of the optical tweezers, in place of the usual Gaussian beam, not only improves the longitudinal optical forces but also exhibits a low sensitivity to the spherical aberration. Now, it remains to carry out in the next Section a comparative analysis of the transverse optical force when the input is a LG_{00}, a LG_{p0} and a $R-LG_{p0}$ beam.

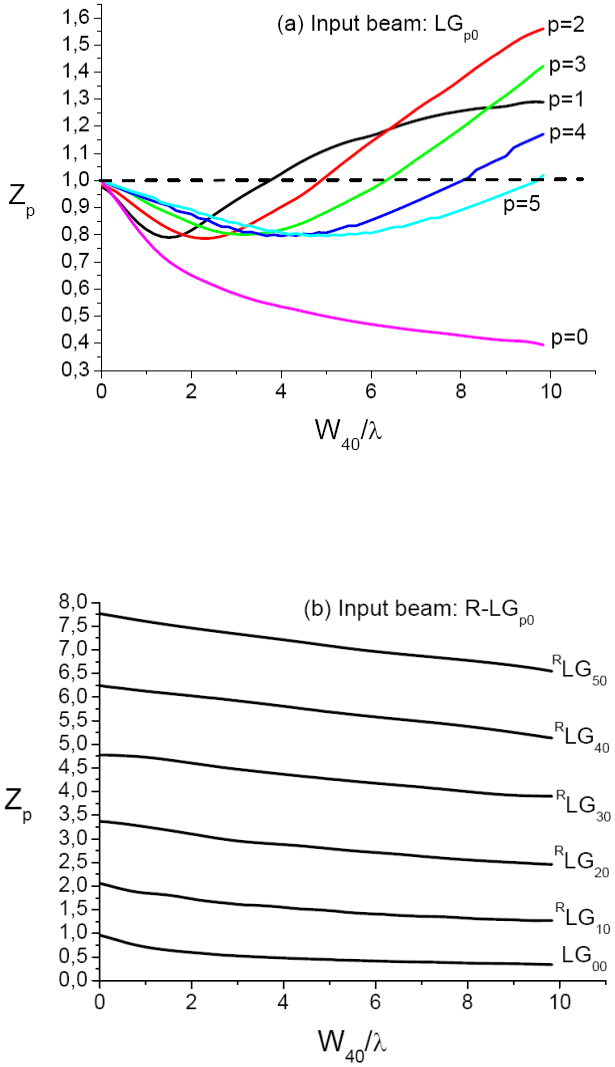

Figure 6: Variations of ratio $Z_p = \{R_F\}_{p>0}^{W_{40}>0} / \{R_F\}_{p=0}^{W_{40}=0}$ versus the spherical aberration coefficient when the input beam is **(a)**: a pure LG_{p0} beam and **(b)**: a rectified LG_{p0} beam.

3.2 Radial optical forces

The radial force exerted by the optical tweezers is proportional to the radial gradient of the intensity profile determined in the plane of the best focus. As in the previous Section, it is convenient to introduce a radial factor of merit noted R_p and defined as follows

$$R_p = \frac{\left\{\vec{\nabla}_r I(r)\Big|_{\max}\right\}_{p\geq 0}^{W_{40}>0}}{\left\{\vec{\nabla}_r I(r)\Big|_{\max}\right\}_{p=0}^{W_{40}=0}} \tag{28}$$

As for the longitudinal forces discussed in Section 3.1, it is easy to interpret the meaning of ratio R_p. The efficiency of the optical trapping radial force, compared to the case of a Gaussian beam enlightening, is improved if $R_p > 1$ and not improved if $R_p < 1$. The results are shown in Fig. 7-a (Fig. 7-b) for the LG_{p0} ($R - LG_{p0}$) beam as input on the focusing lens. It should be recognised the following:

(i) The radial force obtained for a Gaussian input declines relatively rapidly as the spherical aberration is increased. It is observed in Fig. 7-a that the relative variation of R_p for a LG_{00} input is about -56% when the SA coefficient W_{40} varies from 0 to 5λ. Note the same value has been obtained for the decrease of Z_p the longitudinal factor of merit.

(ii) The use of LG_{p0} or $R - LG_{p0}$ beams does not improve the radial force of the optical tweezers since $R_p < 1$.

(iii) It is observed a slight increase (decrease) of R_p when the input is a LG_{p0} ($R - LG_{p0}$) when W_{40} is varied. This result is not surprising given that the mitigation of spherical aberration has been already observed when focusing a rectified LG_{p0} beam [16].

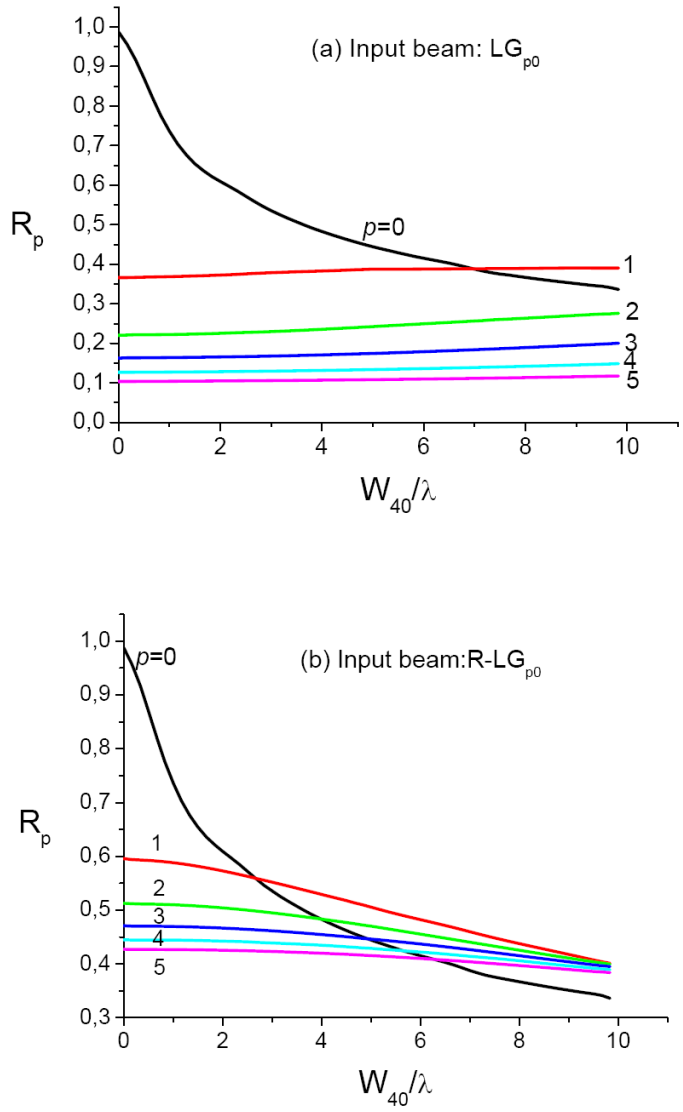

Figure 7: Variations of R_p the radial figure of merit versus the normalised aberration coefficient when the input is **(a)**: a LG_{p0} beam and **(b)**: a rectified LG_{p0} beam.

4. Discussion and conclusion

In summary, we have investigated the influence of spherical aberration upon the performance of optical tweezers enlighten by a Gaussian laser beam. It is observed that a rapid decrease of longitudinal and radial figures of merit occurs, respectively noted Z_0 and R_0, as the spherical aberration is increased. The ratio Z_0 and R_0 show a relative variation of -56% when the

spherical aberration coefficient W_{40} varies from 0 to 5λ. In order to reduce the negative implications of spherical aberrations on the performance of optical tweezers we hypothesised that the possible solution could be the use of a different beam than the usual Gaussian beam as input beam. For that, we selected the rectified LG_{p0} beams which show a certain mitigation of spherical aberration as demonstrated in [16]. We also considered the use of pure (unrectified) LG_{p0} beams. The obtained results show that the radial force exerted by the optical tweezers is not improved when replacing the input Gaussian beam by a LG_{p0} or a rectified LG_{p0} beam. However, the longitudinal factor of merit Z_p (ratio of gradient and scattering forces) of the optical tweezers is greatly increased by a factor varying from (p+1) to (p+2) when the input is a rectified LG_{p0} beam. Contrary to the Gaussian beam, the spherical aberration has a small influence on the longitudinal factor of merit Z_p when the input is a rectified LG_{p0} beam. Note that the Gaussian and LG_{p0} are assumed to carry the same power, and to have the same width based on the second-order intensity moment. Now a question could be raised about the way to force the fundamental mode of a laser to be a single high-order transverse mode LG_{p0}. Such an oscillation can be obtained by inserting a phase [34-36] or amplitude mask [37-41] inside the laser cavity. The action of the phase or amplitude circular masks is to impose the position of the zero of intensity of the desired LG_{p0} mode. Another less known technique for forcing the fundamental mode of a laser to be a pure (single) LG_{p0} mode consists in replacing the cavity rear mirror by a Fox-Smith mirror [42]. In the case where the above intra-cavity techniques would not be practically feasible, it is possible to transform the usual Gaussian beam delivered by the laser outside the cavity into a LG_{p0} mode by using a simple binary diffractive element [43] similar to the device used for rectifying a LG_{p0} beam.

Gaussian, LG_{p0} and rectified LG_{p0} beams are well adapted for trapping particles having a refractive index higher than that of the surrounding medium. Otherwise the trapping laser beam must be hollow when the nanoparticle has a low-refractive index. A peculiar family of such laser beams is the scalar doughnut LG_{0m} beams having the interesting property to carry an orbital angular momentum $\pm m\hbar$ for each photon [44]. Such laser beams are also called as *vortex beams* having a considerable interest in trapping and guiding cold atoms or nanoparticles [45,46]. It should be interesting to examine the influence of a spherical

aberration on optical tweezers performances when the enlightening beam is a vortex beam. It is worthwhile to note that in addition to the above scalar vortex beams there is also the vector vortex beams [47,48] that have the unique characteristic to generate a non-propagating longitudinal electrical field oscillating with the optical frequency in the focal plane [49]. The existence of such longitudinal component together with the presence of a spherical aberration should be an interesting field of investigation for the modelling of optical tweezers based on vector vortex laser beams.

REFERENCES

[1] A. Ashkin, Acceleration and trapping of particles by radiation pressure, Phys. Rev. Lett. **24** (1970) 156-159.

[2] A. Ashkin, J.M. Dziedzic, Optical levitation by radiation pressure, Appl. Phys. Lett. **19** (1971) 282-285.

[3] A. Ashkin, J.M. Dziedzic, J.E. Bjorkholm, S. Chu, Observation of a single-beam gradient force optical trap for dielectric particles, Opt. Lett. **11** (1986) 288-290.

[4] M.J. Padgett, J.E. Molloy, D. McGloin, *Optical Tweezers, Methods and Applications*, CRC Press, Taylor & Francis Group (2010).

[5] H. Jones, O.M. Marago, G. Volpe, *Optical tweezers: Principles and Applications*, Cambridge University Press, UK (2015).

[6] Y. Harada, T. Asakura, Radiation forces on a dielectric sphere in the Rayleigh scattering regime, Opt. Commun. **124** (1996) 529-541.

[7] E. Fällman, O. Axner, Influence of a glass-water interface on the on-axis trapping of micrometer-sized spherical objects by optical tweezers, Appl. Opt. **42** (2003) 3915-3926.

[8] A. Mahmoudi, S.N. Reihani, The effect of immersion oil in optical tweezers, Opt. Express **19** (2011) 14794-14800.

[9] D.G. Abdelsalam, M. Stanislas, Spherical aberration measurement of a microscope objective by used of calibrated spherical particles, Appl. Opt. **56** (2017) 4766-4771.

[10] X.C. Yao, Z.L. Li, H. L. Guo, B.Y. Cheng, D. Z. Zhang, Effects of spherical aberration on optical trapping forces for Rayleigh particles, Chin. Phys. Lett. **18** (2001) 432-434.

[11] A. Rohrbach, E. H. K. Stelzer, Trapping forces, force constants, and potential depths for dielectric spheres in the presence of spherical aberrations, Appl. Opt. **41** (2002) 2494-2507.

[12] C.L. Quesada, J. Andilla, E. Martin-Badosa, Correction of aberration in holographic optical tweezers using a Shack-Hartmann sensor, Appl. Opt. **48** (2009) 1084-1090.

[13] T. Ota, T. Sugiura, S. Kawata, M.J. Booth, M.A. Neil, R. Justaitis, T. Wilson, Enhancement of laser trapping force by spherical aberration correction using a deformable mirror, Jpn. J. Appl. Phys. **42** (2003) 701-703.

[14] E. Theofanidou, L. Wilson, W. J. Hossack, J. Arlt, Spherical aberration correction for optical tweezers, Opt. Commun. **236** (2004) 145-150.

[15] M. C. Zhong, Z. Q. Wang, Y. M. Li, Aberration compensation for optical trapping of cells within living mice, Appl. Opt. **56** (2017) 1972-1976.

[16] S. Haddadi, O. Bouzid, M. Fromager, A. Hasnaoui, A. Harfouche, E. Cagniot, A. Forbes, K. Ait-Ameur, Structured Laguerre-Gaussian beams for mitigation of spherical aberration in tightly focused regimes, J. Opt. **20** (2018) 045602.

[17] S. Quabis, R. Dorn, M. Eberler, O. Glöckl, G. Leuchs, Focusing light to a tighter spot, Opt. Commun. 179 (2000) 1-7.

[18] S. Khonina, A. Ustinov, Increased reverse energy flux area when focusing a linearly polarised annular beam with binary plates, Opt. Lett. **44** (2019) 2008-2011.

[19] H. Ma, Y. Zhang, C. Min, X. Yuan, Controllable propagation and transformation of chiral intensity field at focus, Opt. Lett. **45** (2020) 4823-4826.

[20] J.Pu, H. Zhang, Intensity distribution of Gaussian beams focused by a lens with spherical aberration, Opt. Commun. **151** (1998) 331-338.

[21] G.P. Karman, A.V. Duijl, J.P. Woerdman, Observation of a stronger focus due to spherical aberration, J. Mod. Opt. **45** (1998) 2513-2517.

[22] A. Hasnaoui, A. Bencheikh, K. Ait-Ameur, Tailored TEM_{p0} beams for large sizes 3-D laser prototyping, Opt. Las. Eng. **49** (2011) 248-251.

[23] A. Hasnaoui, A. Bencheikh, M. Fromager, E. Cagniot, K. Ait-Ameur, Creation of a sharper focus by using a rectified TEM_{p0} beam, Opt. Commun. **284** (2011) 1331-1334.

[24] E. Cagniot, M. Fromager, T. Godin, N. Passilly, K. Aït-Ameur, Transverse super-resolution technique involving rectified Laguerre Gaussian LG_{p0} beam, JOSA-A **28** (2011) 1709-1715.

[25] A. Bencheikh, M. Fromager, K. Ait-Ameur, Extended focus depth for Gaussian beam using binary phase diffractive optical elements, Appl. Opt. **57** (2018) 1899-1903.

[26] S. Haddadi, M. Fromager, D. Louhibi, A. Hasnaoui, A. Harfouche, E. Cagniot, K. Ait-Ameur, Improving the intensity of a focused laser beam, Proc. of SPIE **9343** (2015) 93431R-1 to 8.

[27] N.B. Simpson, L. Allen, M.J. Padgett, Optical tweezers and optical spanners with Laguerre-Gaussian modes, J. Mod. Opt. **43** (1996) 2485-2491.

[28] M.A. Clifford, J. Arlt, J. Courtial, K. Dholakia, High-order Laguerre-Gaussian laser modes for studies of cold atoms, Opt. Commun. **156** (1998) 300-306.

[29] J. Arlt, T. Hitomi, K. Dholakia, Atom guiding along Laguerre-Gaussian and Bessel light beams, Appl. Phys. B **71** (2000) 549-554.

[30] W.M. Lee, X.C. Yuan, Observation of three-dimensional optical stacking of microparticles using a single Laguerre-Gaussian beam, Appl. Phys. Lett. **83** (2003) 5124-5126.

[31] P.A. Prentice, M.P. MacDonald, T.G. Frank, A. Cuschieri, G.C. Spalding, W. Sibbett, P.A. Campbell, K. Dholakia, Manipulation and filtration of low index particles with holographic Laguerre-Gaussian optical trap arrays, Opt. Express **12** (2004) 593-600.

[32] V. Garbin, D. Cojoc, E. Ferrari, R.Z. Proietti, S. Cabrini, E.D. Fabrizio, Optical micro-manipulation using Laguerre-Gaussian beams, Jpn. J. Appl. Phys. **44** (2005) 5773-5776.

[33] H.S. Chai, L.G. Wang, Improvement of optical trapping effect by using the focused high-order Laguerre-Gaussian beams, Micron **43** (2012) 887-892.

[34] A.A. Ishaaya, N. Davidson, G. Machavariani, E. Hasman, A.A. Friesem, Efficient selection of high-order Laguerre-Gaussian modes in a Q-switched Nd:YAG Laser, IEEE J. Quantum Electron. **39 (**2003) 74-82.

[35] G. Machavariani, Effects of phase errors on high order mode selection with intracavity phase element, Appl. Opt. **43 (**2004) 6328-6333.

[36] E. Cagniot, M. Fromager, T. Godin, N. Passilly, M. Brunel, K. Aït-Ameur, Variant of the method of Fox&Li dedicated to intracavity laser beam shaping, JOSA A **28** (2011) 489-495.

[37] W.W. Rigrod, Isolation of axi-symmetrical optical-resonator modes, Appl. Phys. Lett. **2** (1963) 51-53.

[38] K.M. Abramski, H.J. Baker, A.D. Colley, R.R. Hall, Single-mode selection using coherent imaging within a slab waveguide CO_2 laser, Appl. Phys. Lett. **60** (1992) 2469-2471.

[39] A. Hasnaoui, K. Aït-Ameur, Properties of a laser cavity containing an absorbing ring Appl. Opt. **49** (2010) 4034-4043.

[40] M. Ciofini, A. Labate, A. Meucci, P.Y. Wang, Experimental evidence of selection and stabilization of spatial patterns in a CO_2 laser by means of spatial perturbations, Opt. Commun. **154** (1998) 307-312.

[41] S. Ngcobo, K. Aït-Ameur, N. Passilly, A. Hasnaoui, A. Forbes, Exciting higher-order radial Laguerre-Gaussian modes in a diode-pumped solid state laser resonator, Appl. Opt. **52** (2013) 2093-2101.

[42] A. Habchi, A. Harfouche, K. Ait-Ameur, Flexible control of laser transverse modes using a Fox-Smith mirror, Appl. Phys. B. **127** (2021) 97.

[43] A. Bencheikh, M. Fromager, K. Aït-Ameur, Generation of Laguerre-Gaussian LGp0 beams using binary phase diffractive optical elements, Appl. Opt. **53** (2014) 4761-4767.

[44] L. Allen, M.W. Beijersbergen, R.J. Speeuw, J.P. Woedman, Orbital angular momentum of light and the transformation of Laguerre-Gauss laser modes, Phys. Rev. A **45** (1992) 8185-8189.

[45] Y. Shen, Y. Meng, X. Fu, M. Gong, Hybrid topological evolution of multi-singularity vortex beams: generalized nature for helical-ince-Gaussian and Hermite-Laguerre-Gaussian modes, J.O.S.A. A **36** (2019) 578-587.

[46] Y. Shen, X. Wang, Z. Xie, C. Min, X. Fu, Q. Liu, M. Gong, X. Yuan, Optical vortices 30 years on: OAM manipulation from topological charge to multiple singularities, Light: Sciences and Applications **8** (2019) article N° 90.

[47] B. Ndagano, I. Nape, M. Cox, C. Rosales-Guzman, A. Forbes, Creation and detection of vector vortex modes for classical and quantum communications, J. Lightwave Technol. **36** (2018) 292-301.

[48] Y. Shen, I. Nape, X. Yang, X. Fu, M. Gong, D. Naidoo, A. Forbes, Creation and control of high-dimensional multi-partite classically entangled light, Light: Sciences and Applications **10** (2021) article N° 50.

[49] D.P. Biss, T.G. Brown, Cylindrical vector beam focusing through a dielectric interface, Opt. Express **9** (2001) 490-497.